ACS APPLIED MATERIALS & INTERFACES

Research Article

www.acsami.org

Mesoporous Polyoxometalate-Based Ionic Hybrid As a Triphasic Catalyst for Oxidation of Benzyl Alcohol with H_2O_2 on Water

Guojian Chen, Yu Zhou, Zhouyang Long, Xiaochen Wang, Jing Li, and Jun Wang*

State Key Laboratory of Materials-Oriented Chemical Engineering, College of Chemistry and Chemical Engineering, Nanjing Tech University, Nanjing 210009, PR China

Supporting Information

ABSTRACT: A self-assembled mesoporous polyoxometalate-based ionic hybrid catalyst $[TMGHA]_{2.4}H_{0.6}PW$ was prepared by combination of alcohol amino-tethered guanidinium ionic liquid [TMGHA]Cl with Keggin phosphotungstic acid $H_3PW_{12}O_{40}$ (PW). Nitrogen sorption experiment validated the formation of mesostructure with moderate BET surface area, and scanning and transmission electron microscopy (SEM and TEM) showed a fluffy coral-shaped morphology for the hybrid. The contact angle test displayed that the hybrid owned hydrophilic−hydrophobic balanced surface that exhibited well wettability for both water and organic substrate like benzyl alcohol. Therefore, the hybrid can efficiently catalyze the water-mediated triphasic oxidation of benzyl alcohol with H_2O_2. During the reaction, the triphase catalytic system showed a special "on water" effect mainly due to the suitable mesostructure and surface wettability, thus providing some clues for the preparation of green heterogeneous catalyst.

KEYWORDS: *polyoxomeatalate, ionic liquid, mesoporous, triphase catalysis, oxidation of alcohols, on water*

1. INTRODUCTION

The development of new green catalytic technology has attracted great attention because of the increasingly energy and environmental crisis, and to a large extent, it depends on the exploration of new catalysts.[1] Heterogeneous catalysts for liquid−liquid−solid (L-L-S) triphase oxidations of organic compounds with pure water as the solvent are important in both academia and chemical industry[2−4] because of the advantages in facile separation of not only the solid catalyst but also the product from the triphasic system, as well as the non-toxic and non-flammable characteristics of the green solvent water. In addition, more than just the role of a solvent, reactivity and selectivity of organic reactions under heterogeneous conditions can be, in some cases, promoted by "on-water" effect.[5] In 2005, Sharpless's group[5] observed that several reactions between water and insoluble organic compounds were dramatically accelerated when carried out in vigorously stirred aqueous suspensions. Subsequently, many on-water reactions, with or without catalyst, emerged endlessly.[6−8] However, water-mediated triphasic reaction systems usually suffer from mass transfer resistance in the interfacial catalysis.[9−12] To overcome this problem, the recent focus is on tuning the mesoporosity and surface wettability of a solid catalyst,[13−15] which is a lively and attractive topic in the area of heterogeneous catalysis.

Polyoxometalates (POMs), a class of transition metal oxygen clusters with tunable rigid structures and redox properties, have been used extensively as efficient catalysts in various oxidation reactions,[16,17] which however suffers from the isolation of those homogeneous POM catalysts. To improve catalyst recovery, many efforts have been made to design POM-based heterogeneous catalysts, in which immobilization of catalytically active species POMs onto various porous supports is the mostly common strategy. The supports include polymers,[18] mesoporous silica,[19] and metal−organic frameworks (MOFs).[20] For water-mediated oxidation of hydrophobic organic substrates, surface modification of the supported POM catalysts are attempted to obtain a hydrophilic−hydrophobic balance inside the catalyst pores, such that exceptional adsorptive and catalytic properties are obtained.[21−24] In addition, self-assembly of POM-anions with appropriate organic cations is another approach for preparing POM-based hybrids, and some of them are heterogeneous catalysts.[25] Taking cationic surfactants as the organic moieties, the obtained surfactant-encapsulated POM-based catalysts usually possess tunable morphologies and hydrophilic/hydrophobic properties, showing enhanced catalytic performances in oxidations of sulfides and alcohols.[26−29] In spite of the fact that high specific surface areas of the heterogeneous POM-derived catalysts would favor the increase of their catalytic activities because of benefits of mass transfer,[30] POM-based ionic hybrids with considerably high surface areas and hydrophilic−hydrophobic balanced surface have not been reported as yet.

On the other hand, ionic liquids (ILs) have attracted increasing attention as reaction media and catalysts in many organic syntheses,[31,32] as well as versatile modifiers for

Received: January 9, 2014
Accepted: March 6, 2014
Published: March 6, 2014

   dx.doi.org/10.1021/am5001757 | ACS Appl. Mater. Interfaces 2014, 6, 4438−4446

improving the surface and electronic properties of various functional materials.[33−35] Particularly, "task-specific" IL cations tethered with functional groups can provide great opportunities for creating diversified ionic liquid-based polyoxometalate (IL-POM) hybrid catalysts *via* the ionic self-assembly strategy.[36−39] In our recent work, a mesoporous IL-POM hybrid catalyst was prepared by employing the dihydroxyl-tethered guanidinium IL-cation, and both dihydroxyl functional group and meso-structure can enhance its catalytic activity in heterogeneous epoxidation of olefin.[40] This encourages us here to design a new self-assembled IL-POM hybrid catalyst $[TMGHA]_{2.4}H_{0.6}PW$ towards the triphase oxidation of benzyl alcohol with H_2O_2 using pure water as the reaction medium (Scheme 1). The hybrid catalyst is prepared by pairing the

Scheme 1. Synthesis of Alcohol Amino Group-Functionalized Guanidinium Polyoxometalate $[TMGHA]_{2.4}H_{0.6}PW$ and $[TMGHA]_{2.4}H_{0.6}PW$-Catalyzed Triphase Oxidation of Benzyl Alcohol with H_2O_2

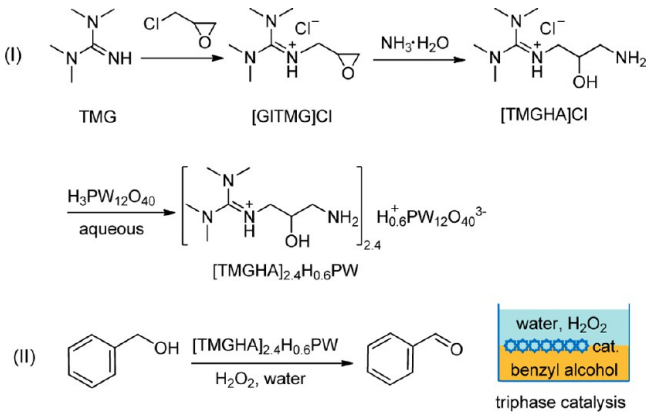

alcohol amino group-functionalized guanidinium cation (TMGHA) with $PW_{12}O_{40}{}^{3-}$ anions (PW), which is fully characterized by ^1H NMR, ^{13}C NMR, elemental analysis, FT-IR, UV−vis, ESR, TG, SEM, TEM, and nitrogen sorption techniques. The hybrid proved to be a mesoporous material with suitable surface wettability and to behave as an efficient triphasic catalyst for water-mediated oxidations of various alcohols with H_2O_2. For comparison, corresponding imidazolium and pyridinium IL-POM counterparts are also prepared and catalytically tested (Supporting Information Scheme S1). A possible on-water interfacial catalysis pathway is proposed for understanding the catalytic behavior.

2. EXPERIMENTAL SECTION

2.1. Materials and Methods. All the chemicals were analytical grade and used as received. FT-IR spectra were recorded on a Nicolet iS10 FT-IR instrument (KBr discs) in the region 4000−400 cm^{-1}. Solid UV−vis spectra were measured with a SHIMADZU UV-260 spectrometer and $BaSO_4$ was used as an internal standard. ESR spectra were recorded on a Bruker EMX-10/12 spectrometer at the X-band. ^1H NMR and ^{13}C NMR spectra were measured with a Bruker DPX 500 spectrometer at ambient temperature in D_2O or D^6-DMSO using TMS as internal reference. The CHN elemental analysis was performed on an elemental analyzer Vario EL cube. X-ray diffraction (XRD) measurements were measured with a SmartLab diffractometer (Rigaku Corporation) equipped with a 9 kW rotating anode Cu source at 40 kV and 200 mA, from 5° to 80° with a scan rate of 0.2° s^{-1}. SEM images were performed on a HITACHI S-4800 field-emission scanning electron microscope and TEM images were obtained by using a JEOL JEM-2010 (200 kV) TEM instrument. BET surface areas were measured at the temperature of liquid nitrogen (77 K) using a BELSORP-MINI analyzer and the samples were degassed at 150 °C for 3 h to a vacuum of 10^{-3} Torr before analysis. Contact angles were measured with a contact angle meter (DropMeter A-100P) at 25 °C. Melting points were measured using an X4 digital microscopic melting point apparatus with an upper limit of 250 °C.

2.2. Catalysts Preparation. The major catalyst in this work, $[TMGHA]_{2.4}H_{0.6}PW$, is synthesized according to the three steps in Scheme 1. First, the glycidyl-tethered tetramethylguanidinium chloride [GlTMG]Cl was synthesized by reaction of *N,N,N′,N′*-tetramethylguanidine (TMG) with epichlorohydrin following our recent work.[40] Next, the alcohol amino group-tethered IL *N″*-(3-amino-2-hydroxypropyl)-*N,N,N′,N′*-tetramethylguanidinium chloride [TMGHA]Cl was prepared by ring-opening reaction of [GlTMG]Cl with aqueous ammonia. In detail, [GlTMG]Cl (1.0 g, 4.8 mmol) was dissolved in water (20 mL), followed with the addition of aqueous ammonia (2.0 g, 14.4 mmol). The obtained mixture was stirred at 60 °C for 24 h in a tightly closed screw-cap flask. After reaction, the excess ammonia and water were removed by distillation at reduced pressure, and then the resultant was dried under vacuum at 70 °C for 12 h to give a light yellow glassy product with a stoichiometric yield. Finally, the hybrid $[TMGHA]_{2.4}H_{0.6}PW$ was prepared by adding [TMGHA]Cl aqueous solution (0.15 mol/L) to the $H_3PW_{12}O_{40}$ aqueous solution (0.05 mol/L) with 3:1 molar ratio and the aqueous suspension was stirred at room temperature for 24 h. The product light yellow precipitate was filtered, washed with water (4 × 20 mL), and dried in a vacuum at 80 °C to give the final product (yield 94%). $[TMGHA]_{2.4}H_{0.6}PW$: Elemental analysis calcd (wt%) C 6.92, H 1.54, N 4.03; Found C 6.90, H 1.45, N 3.94; ^1H NMR (300 MHz, D^6-DMSO, TMS) (Figure S1, Supporting Information) δ 2.90 (s, 12H; N−CH_3), 3.50-4.00 (m, 5H; CH_2, CH), 4.85 (s broad, 1H; OH), 6.19 (s broad, 2H; NH_2), 7.75 ppm (s, 1H; NH); ^{13}C NMR (75.5 MHz, D^6-DMSO, TMS) (Figure S2, Supporting Information) δ 39.50 (N−CH_3), 52.05 (CH_2), 61.09 (CH_2), 67.83 (CH), 160.94 ppm (C═N). FT-IR (ν, KBr) 3436, 2929, 1617, 1560, 1473, 1410, 1080, 979, 896, 808, 595, 519 cm^{-1}.

As a contrast, alcohol amino group-containing imidazolium [MimHA]Cl and pyridinium [PyHA]Cl ILs were synthesized according to the previous literature.[41] The corresponding IL-POMs $[MimHA]_3PW$ and $[PyHA]_3PW$ were prepared similarly as shown in Supporting Information Scheme S1. $[MimHA]_3PW$: Elemental analysis calcd (wt %) C 7.56, H 1.00, N 3.78; Found C 7.60, H 1.38, N 3.67. FT-IR (ν, KBr) 3448, 3151, 1619, 1562, 1449, 1170, 1080, 979, 897, 807, 623, 595 cm^{-1}. $[PyHA]_3PW$: Elemental analysis calcd (wt %) C 8.64, H 1.18, N 2.52; Found C 8.76, H 1.77, N 2.48; FT-IR (ν, KBr) 3563, 3091, 1632, 1497, 1415, 1079, 979, 895, 811, 681, 595 cm^{-1}.

Besides, *N″*-aminoethyl-*N,N,N′,N′*-tetramethylguanidinium bromide [TMGAM]Br was synthesized according to the previous literature.[42] (The details are described in the Supporting Information.) The corresponding amino group-functionalized guanidinium-based POM hybrid $[TMGAM]_{2.1}H_{0.9}PW$ was prepared for comparison. $[TMGAM]_{2.1}H_{0.9}PW$ (white solid, yield 90%): Elemental analysis calcd (wt%) C 5.50, H 1.25, N 3.66; Found: C 5.51, H 1.48, N 3.66; ^1H NMR (300 MHz, D^6-DMSO, TMS) δ 2.67 (m, 2H; CH_2), 2.90 (s, 12H; N−CH_3), 3.10-3.13 (m, 2H; CH_2), 3.35 (s broad, 2H; NH_2), 7.75 ppm (s, 1H; NH); FT-IR (ν, KBr) 3449, 3252, 2963, 1618, 1560, 1459, 1410, 1080, 978, 895, 808, 595, 520 cm^{-1}. In addition, other two control catalysts, TMG-based $[TMG]_3PW$ and monohydroxy-tethered $[TMGOH]_{2.2}H_{0.8}PW$, were prepared according to our recent work.[40] Scheme S2 in the Supporting Information shows the chemical structures of the above three IL-POM hybrids.

Moreover, three different POM anion-paired control catalysts with the same IL-cation, $[TMGHA]_3HSiW$, $[TMGHA]_{2.4}H_{0.6}PMo$, and $[TMGHA]_4HPMoV_2$, were synthesized by employing the corresponding heteropolyacids $H_4SiW_{12}O_{40}$, $H_3PMo_{12}O_{40}$, and $H_5PMo_{10}V_2O_{40}$, respectively. Elemental analysis for $[TMGHA]_3HSiW$ calcd (wt %): C 8.37, H 1.87, N 4.88; Found C 8.24, H 1.98, N 4.72. For $[TMGHA]_{2.4}H_{0.6}PMo$ calcd (wt %): C 10.13, H 2.26, N 5.91; Found C 9.82, H 2.38, N 5.64. For $[TMGHA]_4HPMoV_2$ calcd (wt %): C 15.43, H 3.44, N 8.90; Found C 15.36, H 3.52, N 8.83.

dx.doi.org/10.1021/am5001757 | ACS Appl. Mater. Interfaces 2014, 6, 4438−4446

2.3. Catalytic Tests. The catalytic performance was assessed by the oxidation of various alcohols with H_2O_2 in various reaction media. In a typical run, benzyl alcohol (10 mmol), water (6 mL), and catalyst (0.1 g, 0.03 mmol) were successively added in a reaction tube and stirred at 90 °C for five minutes, and then 30 wt % H_2O_2 (15 mmol) was added drop by drop. The reaction was continued for 6 h with heating at 90 °C with reflux and stirring. For accurate analysis of the product, after reaction ethanol (10 mL) was added to the formed L-L-S triphase system, which immediately turned to a liquid-solid biphasic mixture. The liquid phase was collected, and analyzed by gas chromatography (GC, SP-6890A) equipped with a FID detector and a capillary column (SE-54 30 m × 0.32 mm ×0.3μm). Conversion (based on benzyl alcohol) = mmol (benzyl alcohol) converted/mmol (initial benzyl alcohol) × 100%, selectivity of benzaldehyde = mmol (benzaldehyde) / mmol (benzyl alcohol converted) × 100%. The reaction data were repeated for three times and the error range of the conversions and selectivities was ±2%, mainly because of the GC measurements and experimental operation. To test the catalytic recyclability of $[TMGHA]_{2.4}H_{0.6}PW$, after reaction, the catalyst was separated by filtration, washed with ethanol three times, dried in vacuum at 80 °C for 6 h, and then used for the next run.

3. RESULTS AND DISCUSSION

3.1. Characterization of $[TMGHA]_{2.4}H_{0.6}PW$. For the major IL-POM hybrid sample, the elemental analysis found (wt %) C 6.90, H 1.45, and N 3.94, well corresponding to the calculated values of C 6.92, H 1.54, and N 4.03 based on the formula of $[TMGHA]_{2.4}H_{0.6}PW$. This result suggests that the hybrid is composed of two point four (average value) IL cations of $[TMGHA]^+$ and one $PW_{12}O_{40}^{3-}$ anion, with protons as charge compensation. In addition, the data for ^1H NMR and ^{13}C NMR spectroscopy listed in the Experimental Section confirm the chemical structure of alcohol and amino group-tethered guanidinium-based POM $[TMGHA]_{2.4}H_{0.6}PW$. In the ^1H NMR spectra, the broad signals for $[TMGHA]_{2.4}H_{0.6}PW$ at δ = 4.85 (OH) and δ = 6.19 (NH_2) imply the existence of active protons in the hybrid sample. The TG curve in Figure 1

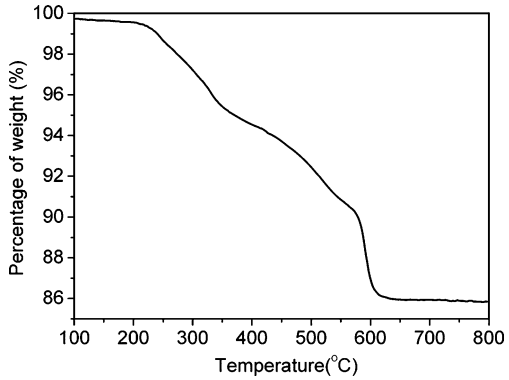

Figure 1. TG curve of the hybrid $[TMGHA]_{2.4}H_{0.6}PW$.

indicates that $[TMGHA]_{2.4}H_{0.6}PW$ possesses a thermally stable structure up to 240 °C. The slight weight loss can be observed at temperature less than 200 °C due to the release of moisture and constitutional water, and the drastic weight loss ranging from 240 to 600 °C is attributed to the decomposition of organic IL-cation moiety plus the subsequent collapse of the inorganic Keggin-type POM structure (forming P_2O_5 and WO_3). The total weight loss is 14.0% in the range of 240−600 °C, consistent with the theoretical data 13.6% on the basis of the formula $[TMGHA]_{2.4}H_{0.6}PW$, once again verifying the rationality of the chemical composition for the hybrid.

Figure 2 illustrates the FT-IR spectra of pure $H_3PW_{12}O_{40}$ and hybrid $[TMGHA]_{2.4}H_{0.6}PW$. Four characteristic vibration

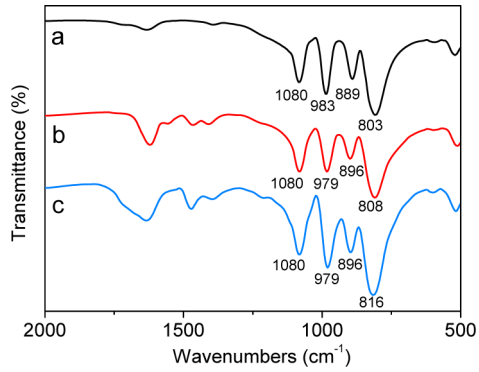

Figure 2. FT-IR spectra of (a) $H_3PW_{12}O_{40}$, (b) the fresh $[TMGHA]_{2.4}H_{0.6}PW$ catalyst, and (c) the recovered $[TMGHA]_{2.4}H_{0.6}PW$.

bands for Keggin structure of $PW_{12}O_{40}^{3-}$ anion are observed for $H_3PW_{12}O_{40}$ at 1080, 983, 889, 803 cm^{-1} (Figure 2, curve a), assignable to the stretching vibration of the central oxygen $\nu(P-O_a)$, terminal oxygen $\nu(W=O_t)$, inter-octahedral oxygen $\nu(W-O_b-W)$, and intra-octahedral oxygen $\nu(W-O_c-W)$, respectively.[43] For $[TMGHA]_{2.4}H_{0.6}PW$ (Figure 2, curve b), the four Keggin featured bands are also observed with only slight shifts, and the peaks located at 1617, 1560, 1473, and 1410 cm^{-1} are assigned to the IL cation TMGHA moiety,[44] indicating the formation of the IL-POM hybrid $[TMGHA]_{2.4}H_{0.6}PW$ via strong ionic bond interactions. The strong broad peak at 3435 cm^{-1} for the stretching vibrations of O−H and N−H indicates the existence of hydroxyl- and amino-containing hydrogen-bonding networks. Both strong ionic bond and hydrogen bond interactions may account for the solid-state of $[TMGHA]_{2.4}H_{0.6}PW$ with a high melting point of approximately 250 °C, and the hybrid is sparingly soluble in DMSO but is insoluble in most common solvents, such as water, alcohols, ethyl acetate, acetic acid, acetone, and acetonitrile. The electronic behavior of $[TMGHA]_{2.4}H_{0.6}PW$ is characterized by UV−vis and ESR spectra, as shown in Figure 3. In the UV−vis spectrum of $[TMGHA]_{2.4}H_{0.6}PW$, the weak broad absorption band (Figure 3A, curve a) ranging from 600 to 800 nm indicates the intramolecular charge transfer from W^{6+} to W^{5+} and the band was undetectable for pure $H_3PW_{12}O_{40}$ (Figure 3A, curve b). The sharp signal at 3500 G for the low-valent W^{5+} species in the ESR spectra (Figure 3B, curve a) is observed for $[TMGHA]_{2.4}H_{0.6}PW$ but not for $H_3PW_{12}O_{40}$ (Figure 3B, curve b). Therefore, both UV−vis and ESR results confirm the coexistence of W^{6+}/W^{5+} in hybrid $[TMGHA]_{2.4}H_{0.6}PW$.[37]

The SEM images of $[TMGHA]_{2.4}H_{0.6}PW$ (Figure 4A, B) show irregular fluffy coral-shaped morphology with micrometer size and nanoscale hollow structure, which may be a reflection of the interconnected IL-POM secondary structure. The TEM images of $[TMGHA]_{2.4}H_{0.6}PW$ (Figure 4C, D) demonstrate the existence of random mesopores among the intertwined particles and micropores among IL-cations and POM-anions. The use of an analogous IL imidazolium cation $[MimHA]^+$ and pyridinium cation $[PyHA]^+$ resulted in the observation of different morphologies for the corresponding IL-POM hybrids $[MimHA]_3PW$ and $[PyHA]_3PW$, as shown in Supporting Information Figure S3. It is seen that $[MimHA]_3PW$ possesses

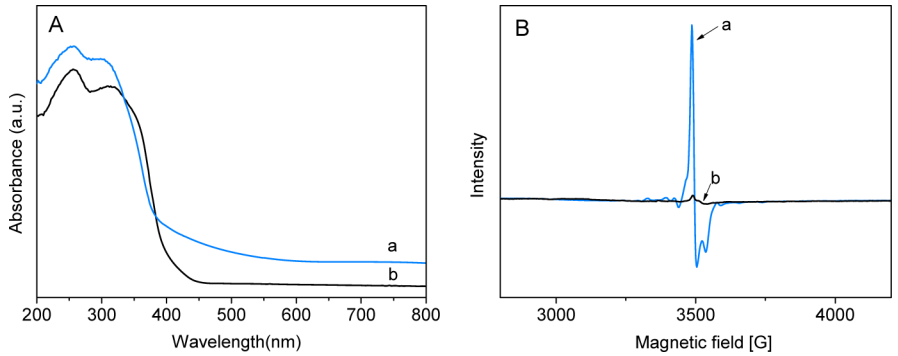

Figure 3. (A) UV−vis and (B) ESR spectra of (a) $[TMGHA]_{2.4}H_{0.6}PW$ and (b) $H_3PW_{12}O_{40}$.

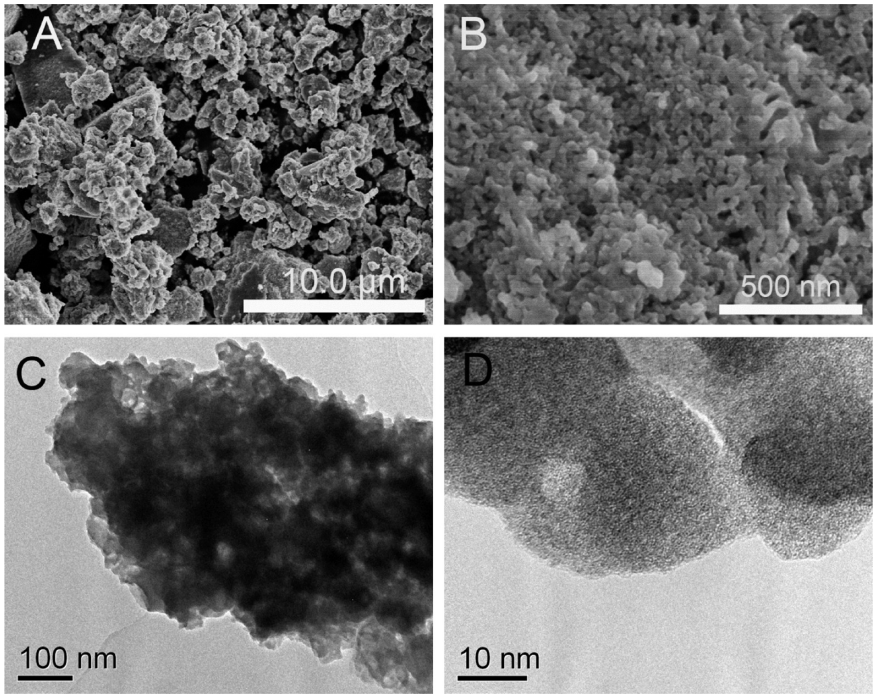

Figure 4. SEM images (A, B) and TEM images (C, D) of $[TMGHA]_{2.6}H_{0.4}PW$.

a flower-like structure with the length on a micrometer scale, which is formed by the packing of nanoscale primary particles, while $[PyHA]_3PW$ changes to random close-packed blocks at the micrometer level.

The XRD patterns of pure $H_3PW_{12}O_{40}$ and the hybrid $[TMGHA]_{2.4}H_{0.6}PW$ are illustrated in Figure 5. The characteristic sharp Bragg peaks observed for Keggin-type $H_3PW_{12}O_{40}$ disappears in the case of $[TMGHA]_{2.4}H_{0.6}PW$. For the latter, only a new broad Bragg peak is detected at $2\theta = 8.0°$ with a d spacing of 1.1 nm, very close to the theoretical size of a primary structural unit of IL-POM ionic hybrid. This phenomenon also corresponds to the observed result from the high resolution TEM image (Figure 4D), which the primary structural units (~1.1 nm) are clearly observed throughout the IL-POM secondary structure. As a result, the hybrid $[TMGHA]_{2.4}H_{0.6}PW$ possesses a non-crystal structure but with certain regular ion-pair array.[45]

The specific Brunauer−Emmett−Teller (BET) surface areas and porous structures of $[TMGHA]_{2.4}H_{0.6}PW$ and the IL-POM analogues are characterized by nitrogen sorption experiments. As shown in Figure 6A, the nitrogen sorption isotherms of $[TMGHA]_{2.4}H_{0.6}PW$ (curve a) and $[MimHA]_3PW$ (curve b)

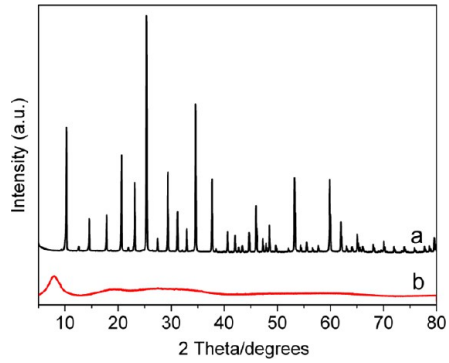

Figure 5. XRD patterns of (a) $H_3PW_{12}O_{40}$ and (b) $[TMGHA]_{2.4}H_{0.6}PW$.

are type IV with a clear H1-type hysteresis loop in the relative pressure P/P_0 ranging from 0.8 to 0.9, indicating the formation of mesoporous materials. The Barrett−Joyner−Halenda (BJH) pore size distribution curves in Figure 4B give the most probable pore sizes centered at 16.0 and 37.9 nm for $[TMGHA]_{2.4}H_{0.6}PW$ and $[MimHA]_3PW$, respectively. In

dx.doi.org/10.1021/am5001757 | ACS Appl. Mater. Interfaces 2014, 6, 4438−4446

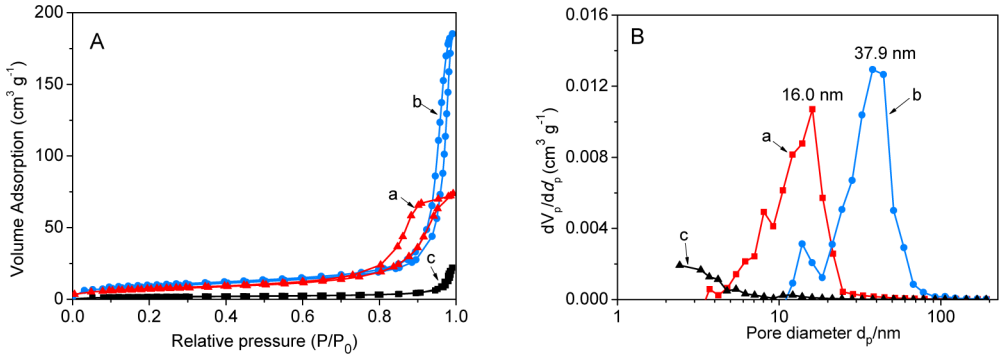

Figure 6. (A) N_2 adsorption-desorption isotherms and (B) BJH pore size distributions of (a) $[TMGHA]_{2.4}H_{0.6}PW$, (b) $[MimHA]_3PW$, and (c) $[PyHA]_3PW$.

contrast, the nitrogen sorption result for $[PyHA]_3PW$ is indicative of a nonporous solid (Figure 6, curve c). Table 1 lists the data of BET surface areas, pore volumes, and average pore sizes. The results indicate that $[TMGHA]_{2.4}H_{0.6}PW$ has a moderate BET surface area of 25.0 m^2 g^{-1} with a pore volume of 0.11 cm^3 g^{-1}, similar to the results of $[TMGDH]_3PW$ in our recent work.[40] Also, the control catalyst $[MimHA]_3PW$ has a higher BET surface area of 31.9 m^2 g^{-1} with a large average mesopore size of 43.9 nm and total pore volume of 0.35 cm^3 g^{-1}, matching up to previously reported POM-based mesoporous hybrid materials specially modified by macrocations.[46,47]

Table 1. Textural Parameters of Various IL-POM Samples

IL-POM samples	S_{BET}[a] (m^2 g^{-1})	V_p[b] (cm^3 g^{-1})	D_{av}[c] (nm)
$[TMGHA]_{2.4}H_{0.6}PW$	25.0	0.11	18.1
$[MimHA]_3PW$	31.9	0.35	43.9
$[PyHA]_3PW$	6.2	0.01	6.4

[a]BET surface area. [b]Total pore volume. [c]Average pore size.

The low BET surface area of 6.2 m^2 g^{-1} for $[PyHA]_3PW$ is consistent with the low surface areas (<10 m^2 g^{-1}) for common organic POM salts. As a result, we obtain two mesoporous IL-POM hybrid catalysts with moderate BET surface areas.

Figure 7 shows the surface wettability of $[TMGHA]_{2.4}H_{0.6}PW$ and its analogues. When a water droplet contacts the sheet of $[TMGHA]_{2.4}H_{0.6}PW$, it yields a contact angle of 73° (Figure 7A), implying its moderate hydrophilicity. For the analogue samples $[MimHA]_3PW$ and $[PyHA]_3PW$ with the IL-cation changed (Figure 7B, C), slightly lowered contact angles 68° and 69° are detected, indication similar hydrophilicity. With benzyl alcohol as the testing droplet, Figure 7D–F show contacted angles of 12–15° on the surfaces of three IL-POM hybrids, demonstrating good surface wettability for benzyl alcohol.[48] Therefore, the hybrid $[TMGHA]_{2.4}H_{0.6}PW$ shows good wettability for both water and alcohol, which is the substrate for the oxidation reaction below.

3.2. Catalytic Assessment. The catalytic performances of different IL-POM materials are assessed in the oxidation of benzyl alcohol with H_2O_2 in aqueous media, and the results are

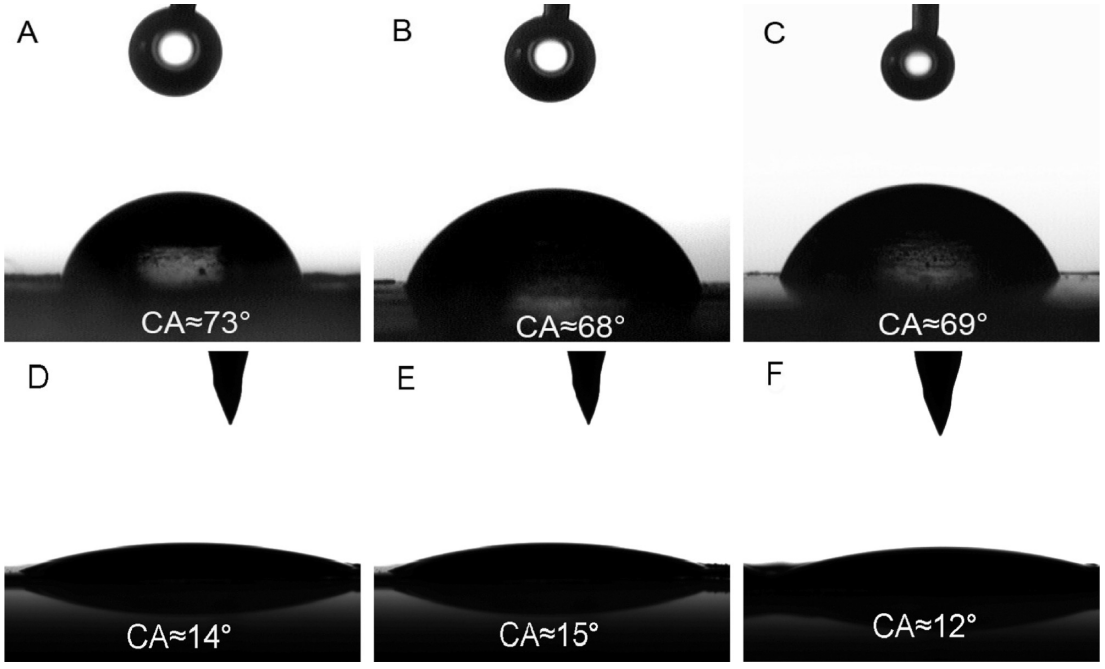

Figure 7. Contact angles of water droplets on the surface of (A) $[TMGHA]_{2.4}H_{0.6}PW$, (B) $[MimHA]_3PW$ and (C) $[PyHA]_3PW$; contact angles of benzyl alcohol droplets on the surface of (D) $[TMGHA]_{2.4}H_{0.6}PW$, (E) $[MimHA]_3PW$ and (F) $[PyHA]_3PW$.

dx.doi.org/10.1021/am5001757 | ACS Appl. Mater. Interfaces 2014, 6, 4438–4446

Table 2. Catalytic Performances of Various POM Catalysts and Effect of Solvent for Oxidation of Benzyl Alcohol with H_2O_2[a]

entry	catalyst	reaction solvent	reaction system[b]	conversion[c](%)	selectivity[d] (%)	yield[e] (%)
1	none	water	L-L	6.0	100	6.0
2	$H_3PW_{12}O_{40}$	water	L-L	97.0	92.4	89.6
3	$[TMGHA]_{2.4}H_{0.6}PW$	water	L-L-S	97.9	93.5	91.5
4	$[TMGHA]_{2.4}H_{0.6}PW$	ethanol	L-S	59.2	96.6	57.2
5	$[TMGHA]_{2.4}H_{0.6}PW$	*tert*-butanol	L-S	80.5	96.7	77.8
6	$[TMGHA]_{2.4}H_{0.6}PW$	acetonitrile	L-S	69.8	91.8	64.1
7	$[TMGHA]_{2.4}H_{0.6}PW$	toluene	L-S	65.4	98.9	64.7
8	$[TMGHA]_{2.4}H_{0.6}PW$	ethanol/water	L-S	72.9	99.2	72.3
9	$[TMGHA]_{2.4}H_{0.6}PW$	*tert*-butanol/water	L-S	91.1	94.2	85.8
10	$[TMGHA]_{2.4}H_{0.6}PW$	acetonitrile/water	L-S	98.7	91.7	90.5
11	$[TMGHA]_{2.4}H_{0.6}PW$	toluene/water	L-L-S	93.6	97.8	91.6
12	$[TMG]_3PW$	water	L-L	90.1	89.8	83.8
13	$[TMGOH]_{2.2}H_{0.8}PW$	water	L-L	90.6	89.2	80.8
14	$[TMGAM]_{2.1}H_{0.9}PW$	water	L-L	96.3	89.7	86.4
15	$[MimHA]_3PW$	water	L-L-S	95.5	95.4	91.1
16	$[PyHA]_3PW$	water	L-L-S	72.8	95.8	69.7
17	$[TMGHA]_3HSiW$	water	L-L-S	16.1	99.5	16.0
18	$[TMGHA]_{2.4}H_{0.6}PMo$	water	L-L-S	74.2	92.4	68.6
19	$[TMGHA]_4HPMoV_2$	water	L-L-S	28.9	99.0	28.6

[a]Reaction conditions: benzyl alcohol (10 mmol), 30 wt % H_2O_2 (15 mmol), catalyst (0.03 mmol), solvent (6 mL, water or volume ratio for organic solvent/water 1:1), 90 °C, 6 h. [b]L (liquid, water phase), L (liquid, organic phase), and S (solid, catalyst). [c]Conversion based on benzyl alcohol. [d]Selectivity for benzaldehyde (by-product benzoic acid). [e]Yield (%) = conversion × selectivity ×100%.

summarized in Table 2. The benzyl alcohol conversion is as low as 6.0% in the absence of a catalyst (entry 1). Neat $H_3PW_{12}O_{40}$ exhibits a high catalytic activity with the conversion of 97.7% and selectivity of 92.4%, with the yield of 89.6% (entry 2). The $H_3PW_{12}O_{40}$-catalyzed reaction presents a liquid−liquid (L-L) biphasic system because of the well solution of the catalyst and poor solubility of benzyl alcohol in aqueous media.[49,50] In contrast, $[TMGHA]_{2.4}H_{0.6}PW$ is a heterogeneous catalyst for this reaction and exhibits higher conversion of 97.9% and selectivity of 93.5%, with a yield of 91.5% (entry 3). This result is obtained under the optimized condition after the detailed investigations of various reaction parameters including the amounts of catalyst and water, reaction time, and molar ratio of H_2O_2 to benzyl alcohol, as shown in Supporting Information Figure S4. In this case, the reaction mixture turns out to be L-L-S triphase because of the insolubility of the solid hybrid and the immiscibility between water and benzyl alcohol. Figure 8 displays the photographs of the reaction process at different stages. Before the onset of the reaction, the powdered catalyst $[TMGHA]_{2.4}H_{0.6}PW$ is placed at the bottom of the immiscible water−oil biphase, and the hardly soluble property of the hybrid is observed even at 90 °C. During the reaction, the catalyst powder is well dispersed in liquid mixture of water and organic substrate, in other words, the reaction takes place in aqueous suspensions, which consists with an "on water" catalytic system.[51] At the end of reaction with a stop of stir, self-separation of the three phases occurs immediately, forming a clearly observed L-L-S triphase: the solid catalyst is well suspended at the interfacial zone between the upper layer of water and the bottom layer of oil. This triphasic system may cause facile separation of product and easy recovery of the catalyst. The influence of the amount of water added in this reaction is thus investigated (Supporting Information Figure S4D). Under solvent-free condition, modest conversion of 82.5% and low selectivity of 81.0% are observed. Interestingly, both conversion and selectivity dramatically increase up to 95.1% and 90.4% with adding 2 mL water into the reaction, and the maximum values are achieved by adding 6 mL water. However, the conversion and yield slightly decrease with adding much more water. These observations indicate that the volume of water is a crucial parameter for determining the performance of the catalyst in the triphase alcohol oxidation.

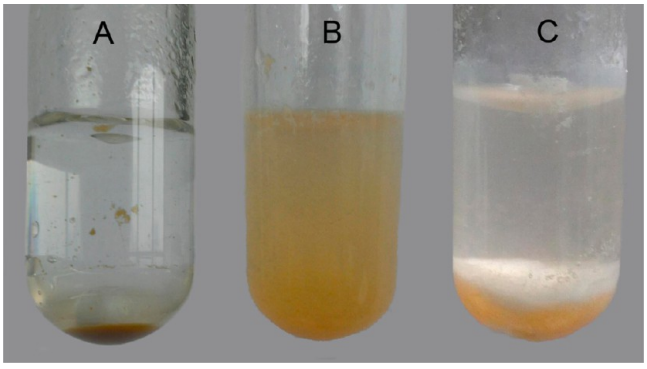

Figure 8. Photographs of water-mediated oxidation of benzyl alcohol with H_2O_2 catalyzed by $[TMGHA]_{2.4}H_{0.6}PW$. (A) Before mixing: Upper layer water, middle layer oil, and bottom catalyst power. (B) during reaction: The powdered catalyst is well-dispersed in liquid mixture. (C) After reaction: Upper layer water, bottom layer oil, and in-between solid catalyst.

To further explore the above promotional effect of water, various organic solvents, and organic solvent/water cosolvents (volume ratio 1:1) are employed. The organic solvents include ethanol, *tert*-butanol, acetonitrile, and toluene, and they well dissolve the substrate benzyl alcohol; however, the catalyst $[TMGHA]_{2.4}H_{0.6}PW$ is still insoluble in these organic solvents, causing liquid−solid (L-S) systems. Nonetheless, the resulting L-S biphasic reactions only give lower conversions of 60−80% (entries 4−7, Table 2), in agreement with previous observations using organic solvents.[52] By contrast, the conversions are enhanced dramatically with the cosolvents of organic solvent/water (entries 8-11). It is worth noting that the

cosolvents of acetonitrile/water and toluene/water provide yields of 90.5% and 91.6%, comparable to that of pure water solvent. The phenomenon validates the significant role of water in enhancing the activity of the triphasic catalyst $[TMGHA]_{2.4}H_{0.6}PW$.

Besides $[TMGHA]_{2.4}H_{0.6}PW$, the control catalysts with other IL cations are also tested in the oxidation of benzyl alcohol. As shown in Table 2, the catalyst $[TMG]_3PW$ without a functional group tethered to tetramethylguanidinium (TMG) is dissolved in the reaction, presenting a yield of 83.8% (entry 12). When the tethered functional group is either single hydroxyl (−OH) or amino ($-NH_2$), the resulting catalysts $[TMGOH]_{2.2}H_{0.8}PW$ and $[TMGAM]_{2.1}H_{0.9}PW$ are still homogeneous, showing the yields of 80.8% and 86.4%, respectively (entries 13 and 14). The catalytic performances of these three catalysts are much inferior than the heterogeneous catalyst $[TMGHA]_{2.4}H_{0.6}PW$ containing the alcohol amino group-containing TMG cation. This comparison suggest that the coexistence of −OH and $-NH_2$ groups in TMG cation is not only crucial for the heterogenization process but also for the higher catalytic performance. Moreover, the analogues $[MimHA]_3PW$ and $[PyHA]_3PW$ prepared with alcohol amino group-containing pyridinium and imidazolium cations give rise to the same triphase reaction process as $[TMGHA]_{2.4}H_{0.6}PW$ does, which confirms the important role of the tethered alcohol amino group in forming their heterogeneous nature. Though $[MimHA]_3PW$ and $[PyHA]_3PW$ display similar surface wettability as mentioned above, they exhibit different catalytic activities: mesoporous $[MimHA]_3PW$ shows a benzaldehyde yield of 91.1% (entry 15), as high as $[TMGHA]_{2.4}H_{0.6}PW$, while nonporous $[PyHA]_3PW$ gives a low yield of 69.7% (entry 16).

For comparing various heteropolyanions, $[TMGHA]_3HSiW$, $[TMGHA]_{2.4}H_{0.6}PMo$, and $[TMGHA]_4HPMoV_2$ are synthesized with the same IL cation $[TMGHA]^+$. They are also heterogeneous catalysts because of insoluble properties throughout the reaction, but show lower conversions of 16.1%, 74.2%, and 28.9%, respectively (entries 17−19). The lower activities compared with the PW-paired $[TMGHA]_{2.4}H_{0.6}PW$ are similar to the results in our previous report.[53] Therefore, the commercial PW anion-based catalyst $[TMGHA]_{2.4}H_{0.6}PW$ is a highly efficient catalyst for water-mediated oxidation of benzyl alcohol with H_2O_2. Besides, towards other typical alcohol substrates (Table S1, Supporting Information), $[TMGHA]_{2.4}H_{0.6}PW$ also presents well triphase catalytic performances for 1-phenylethyl alcohol, benzhydrol, and cyclohexanol, suggesting that the catalyst $[TMGHA]_{2.4}H_{0.6}PW$ is also applicable to water-mediated oxidations of aromatic and cyclic alcohols.

Previously, the water-mediated triphase oxidation of benzyl alcohol with H_2O_2 has also been reported over mesoporous silica and magnetic nanoparticles supported tungstate-based POM catalysts.[19,22,54] Compared with them, the present self-assembled mesoporous IL-POMs show higher activities under milder conditions. To assess catalytic reusability, $[TMGHA]_{2.4}H_{0.6}PW$ was recovered simply by filtration and then reused for the next run without adding any fresh catalyst. Supporting Information Figure S5 displays the result of the five-run recycling test. Only a very slow decrease of conversion is observed in the recycling runs, implying good potential for catalyst reuse. Further, the elemental analysis (wt %) for the recovered catalyst is C 7.12, H 1.65, N 4.05, very close to the data for the fresh catalyst. In addition, the recycled catalyst also shows similar IR spectrum (Figure 2, curve c) as the fresh one. Four characteristic bands for Keggin $PW_{12}O_{40}^{3-}$ are retained, and no obvious new peak is detected. The hydroxyl groups attached to the mesoporous hybrid $[TMGHA]_{2.4}H_{0.6}PW$ are hardly oxidized to C═O under the experimental conditions, which attributes to its inherent inertness of β-hydroxyl within the glycerol-derived structures.[55] As a result, the above elemental analysis and IR spectrum experiments indicate that the structure of the recovered catalyst is well preserved.

3.3. Insight into Catalytic Behavior of $[TMGHA]_{2.4}H_{0.6}PW$. As demonstrated above, the mesoporous $[TMGHA]_{2.4}H_{0.6}PW$ with dual wettability for water and benzyl alcohol behaves as a triphasic catalyst and shows a higher activity than the biphasic systems using organic solvents. Therefore, the triphase catalysis seems to take place on water. Scheme 2 illustrates the proposed on-water catalytic reaction route. In the reaction, water and H_2O_2 are chemisorbed on the hydrophilic surface enriched with hydroxyl and amino groups in IL cations of the catalyst, forming a H_2O_2-containing water layer on catalyst surface.[56,57] Previous studies indicate that about 25% of surface water molecules at hydrophobic interface have dangling −OH groups where the H atom is no long hydrogen-bonded to other H_2O.[58] Consequently, the dangling −OH groups at oil−water interface play a role of the H-bond donor to promote the interactions between the substrate (benzyl alcohol) and water, which accelerates the kinetics of on water catalysis.[57,58] On the basis of this suggestion, benzyl alcohol molecules diffuse into the water layer via the formation of hydrogen bonding between the dangling $-OH/-NH_2$ groups and alcohol. The diffused alcohols are then attacked by the catalytically active species $\{PO_4[WO(O_2)_2]_4\}^{3-}$ which are formed by the interaction of H_2O_2 with $PW_{12}O_{40}^{3-}$,[59,60] and the catalysis is closed by the generation of the product benzaldehyde. Benzaldehyde could be timely expelled from water layer, avoiding further oxidation and benefiting high selectivity. In above process, the suitable surface microenvironment for $[TMGHA]_{2.4}H_{0.6}PW$ with dual wettability for water and benzyl alcohol is the key factor. Besides, the mesostructure with a considerably high surface area allowing fast mass-transfer should be a prerequisite for a heterogeneous catalyst to make a full play of the above on-water catalysis route, which is demonstrated by another similarly active catalyst $[MimHA]_3PW$. Notably, the rationality of this proposal is also reflected by the contrastive nonporous $[PyHA]_3PW$ with low surface area and low activity.

Scheme 2. Proposed On-Water Catalytic Reaction Route for the Oxidation of Benzyl Alcohol with H_2O_2 over the Catalyst $[TMGHA]_{2.4}H_{0.6}PW$

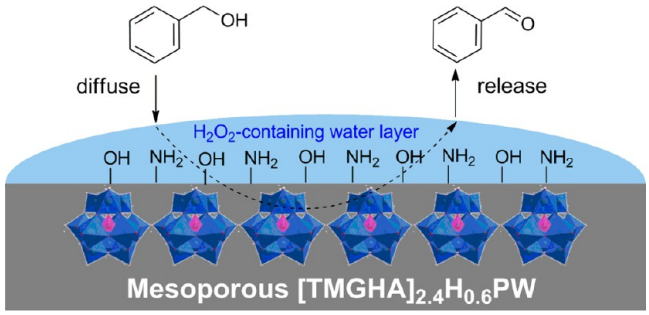

dx.doi.org/10.1021/am5001757 | ACS Appl. Mater. Interfaces 2014, 6, 4438−4446

4. CONCLUSIONS

We develop the mesoporous polyoxometalate-based ionic hybrid $[TMGHA]_{2.4}H_{0.6}PW$ for catalyzing water-mediated triphase oxidations of alcohols with H_2O_2. The hybrid is synthesized by finely designing the ionic liquid cation of tetramethylguanidinium functionalized with hydroxyl and amino groups, and the self-assembly of that cation with the Keggin phosphotungstic anion. The high activity of the hybrid catalyst associates to its mesoporosity and dual wettability for water and alcohols. An on-water catalysis route is suggested to understand the superior catalytic performance. The self-assembling synthesis strategy in this work may provide an efficient and facile way to fabricate highly efficient triphasic hybrid catalysts for organic oxidations using pure water medium.

■ ASSOCIATED CONTENT

Supporting Information

Schemes S1 and S2 show the synthesis and chemical structures of the analogous IL-POM catalysts; Figures S1 and S2 show the ^1H NMR and ^{13}C NMR spectra for $[TMGHA]_{2.4}H_{0.6}PW$; Figure S3 displays the SEM images of $[MimHA]_3PW$ and $[PyHA]_3PW$; Figure S4 and S5 show reaction parameters and recycling experiments in the oxidation of benzyl alcohol. Table S1 shows the catalytic performances of other alcohol substrates. This material is available free of charge via the Internet at http://pubs.acs.org.

■ AUTHOR INFORMATION

Corresponding Author

*Tel: +86-25-83172264. Fax: +86-25-83172261. E-mail: junwang@njtech.edu.cn.

Notes

The authors declare no competing financial interest.

■ ACKNOWLEDGMENTS

The authors thank greatly the National Natural Science Foundation of China (Nos. 21136005 and 21303084), Jiangsu Provincial Science Foundation for Youths (No. BK20130921), and the Scientific Research and Innovation Project for College Graduates of Jiangsu Province (CXZZ13_0447).

■ REFERENCES

(1) Sheldon, R. A. Fundamentals of Green Chemistry: Efficiency in Reaction Design. *Chem. Soc. Rev.* **2012**, *41*, 1437−1451.
(2) Regen, S. L. Triphase Catalysis. *Angew. Chem., Int. Ed. Engl.* **1979**, *18*, 421−429.
(3) Tundo, P.; Perosa, A. Multiphasic Heterogeneous Catalysis Mediated by Catalyst-Philic Liquid Phases. *Chem. Soc. Rev.* **2007**, *36*, 532−550.
(4) Simon, M.-O.; Li, C.-J. Green Chemistry Oriented Organic Synthesis in Water. *Chem. Soc. Rev.* **2012**, *41*, 1415−1427.
(5) Narayan, S.; Muldoon, J.; Finn, M. G.; Fokin, V. V.; Kolb, H. C.; Sharpless, K. B. "On Water": Unique Reactivity of Organic Compounds in Aqueous Suspension. *Angew. Chem., Int. Ed.* **2005**, *44*, 3275−3279.
(6) Butler, R. N.; Coyne, A. G. Water: Nature's Reaction Enforcer—Comparative Effects for Organic Synthesis "In-Water" and "On-Water. *Chem. Rev.* **2010**, *110*, 6302−6337.
(7) Gawande, M. B; Bonifácio, V. D. B.; Luque, R.; Branco, P. S.; Varma, R. S. Benign by Design: Catalyst-Free In-Water, On-Water Green Chemical Methodologies in Organic Synthesis. *Chem. Soc. Rev.* **2013**, *42*, 5522−5551.
(8) Rezaeifard, A.; Haddad, R.; Jafarpour, M.; Hakimi, M. Catalytic Epoxidation Activity of Keplerate Polyoxomolybdate Nanoball toward Aqueous Suspension of Olefins under Mild Aerobic Conditions. *J. Am. Chem. Soc.* **2013**, *135*, 10036−10039.
(9) Regen, S. L.; Besse, J. J. Liquid-Solid-Liquid Triphase Catalysis. Consideration of the Rate-Limiting Step, Role of Stirring, and Catalyst Efficiency for Simple Nucleophilic Displacement. *J. Am. Chem. Soc.* **1979**, *101*, 4059−4063.
(10) Nur, H.; Ikeda, S.; Ohtani, B. Phase-Boundary Catalysis of Alkene Epoxidation with Aqueous Hydrogen Peroxide using Amphiphilic Zeolite Particles Loaded with Titanium Oxide. *J. Catal.* **2001**, *204*, 402−408.
(11) Choi, K.; Ikeda, S.; Ishino, S.; Ikeue, K.; Matsumura, M.; Ohtani, B. Oxidation of Hydrophobic Alcohols using Aqueous Hydrogen Peroxide over Amphiphilic Silica Particles Loaded with Titanium(IV) Oxide as a Liquid−Liquid Phase-Boundary Catalyst. *Appl. Catal., A* **2005**, *278*, 269−274.
(12) Yuan, L.; Razali, R.; Efendi, J.; Buang, N. A.; Nur, H. Temperature-Controlled Selectivity in Oxidation of 1-Octene by Using Aqueous Hydrogen Peroxide in Phase-Boundary Catalytic System. *Appl. Catal., A* **2013**, *46*, 21−25.
(13) Wu, D.; Xu, F.; Sun, B.; Fu, R.; He, H.; Matyjaszewski, K. Design and Preparation of Porous Polymers. *Chem. Rev.* **2012**, *112*, 3959−4015.
(14) Cordeiro, P. J.; Tilley, T. D. Enhancement of the Catalytic Activity of Titanium-Based Terminal Olefin Epoxidation Catalysts via Surface Modification with Functionalized Protic Molecules. *ACS Catal.* **2011**, *1*, 455−467.
(15) Wang, M.; Wang, F.; Ma, J.; Chen, C.; Shi, S.; Xu, J. Insights into Support Wettability in Tuning Catalytic Performance in the Oxidation of Aliphatic Alcohols to Acids. *Chem. Commun.* **2013**, *49*, 6623−6625.
(16) Long, D.; Burkholder, E.; Cronin, L. Polyoxometalate Clusters, Nanostructures and Materials: From Self Assembly to Designer Materials and Devices. *Chem. Soc. Rev.* **2007**, *36*, 105−121.
(17) Mizuno, N.; Yamaguchi, K.; Kamata, K. Epoxidation of Olefins with Hydrogen Peroxide Catalyzed by Polyoxometalates. *Coord. Chem. Rev.* **2005**, *249*, 1944−1956.
(18) Maradur, S. P.; Jo, C.; Choi, D. H.; Kim, K.; Ryoo, R. Mesoporous Polymeric Support Retaining High Catalytic Activity of Polyoxotungstate for Liquid-Phase Olefin Epoxidation using H_2O_2. *ChemCatChem* **2011**, *3*, 1435−1438.
(19) Zhang, R.; Ding, W.; Tu, B.; Zhao, D. Mesoporous Silica: An Efficient Nanoreactor for Liquid-Liquid Biphase Reactions. *Chem. Mater.* **2007**, *19*, 4379−4381.
(20) Corma, A.; García, H.; Xamena, F. X. L. Engineering Metal Organic Frameworks for Heterogeneous Catalysis. *Chem. Rev.* **2010**, *110*, 4606−4655.
(21) Doherty, S.; Knight, J. G.; Ellison, J. R.; Weekes, D.; Harrington, R. W.; Hardacre, C.; Manyar, H. An Efficient Recyclable Peroxometalate-Based Polymer-Immobilised Ionic Liquid Phase (PIILP) Catalyst for Hydrogen Peroxide-Mediated Oxidation. *Green Chem.* **2012**, *14*, 925−929.
(22) Tan, R.; Liu, C.; Feng, N.; Xiao, J.; Zheng, W.; Zheng, A.; Yin, D. Phosphotungstic Acid Loaded on Hydrophilic Ionic Liquid Modified SBA-15 for Selective Oxidation of Alcohols with Aqueous H_2O_2. *Microporous Mesoporous Mater.* **2012**, *158*, 77−87.
(23) Han, Q.; He, C.; Zhao, M.; Qi, B.; Niu, J.; Duan, C. Engineering Chiral Polyoxometalate Hybrid Metal-Organic Frameworks for Asymmetric Dihydroxylation of Olefins. *J. Am. Chem. Soc.* **2013**, *135*, 10186−10189.
(24) Li, D.; Yin, P.; Liu, T. Supramolecular Architectures Assembled from Amphiphilic Hybrid Polyoxometalates. *Dalton Trans.* **2012**, *41*, 2853−2861.
(25) Mizuno, N.; Yamaguchi, K.; Kamata, K. Molecular Design of Polyoxometalate-Based Compounds for Environmentally-Friendly Functional Group Transformations: From Molecular Catalysts to Heterogeneous Catalysts. *Catal. Surv. Asia* **2011**, *15*, 68−79.

(26) Nisar, A.; Wang, X. Surfactant-Encapsulated Polyoxometalate Building Blocks: Controlled Assembly and Their Catalytic Properties. *Dalton Trans.* **2012**, *41*, 9832−9845.
(27) Nisar, A.; Zhuang, J.; Wang, X. Construction of Amphiphilic Polyoxometalate Mesostructures as a Highly Efficient Desulfurization Catalyst. *Adv. Mater.* **2011**, *23*, 1130−1135.
(28) Nisar, A.; Lu, Y.; Zhuang, J.; Wang, X. Polyoxometalate Nanocone Nanoreactors: Magnetic Manipulation and Enhanced Catalytic Performance. *Angew. Chem., Int. Ed.* **2011**, *50*, 3187−3192.
(29) Jing, L.; Shi, J.; Zhang, F.; Zhong, Y.; Zhu, W. Polyoxometalate-Based Amphiphilic Catalysts for Selective Oxidation of Benzyl Alcohol with Hydrogen Peroxide under Organic Solvent-Free Conditions. *Ind. Eng. Chem. Res.* **2013**, *52*, 10095−10104.
(30) Mizuno, N.; Misono, M. Heterogeneous Catalysis. *Chem. Rev.* **1998**, *98*, 199−218.
(31) Hallett, J. P.; Welton, T. Room-Temperature Ionic Liquids: Solvents for Synthesis and Catalysis. 2. *Chem. Rev.* **2011**, *111*, 3508−3576.
(32) Zhang, Q.; Zhang, S.; Deng, Y. Recent Advances in Ionic Liquid Catalysis. *Green Chem.* **2011**, *13*, 2619−2637.
(33) Yamaguchi, K.; Yoshida, C.; Uchida, S.; Mizuno, N. Peroxotungstate Immobilized on Ionic Liquid-Modified Silica as a Heterogeneous Epoxidation Catalyst with Hydrogen Peroxide. *J. Am. Chem. Soc.* **2005**, *127*, 530−531.
(34) Zhang, Y.; Shen, Y.; Yuan, J.; Han, D.; Wang, Z.; Zhang, Q.; Niu, L. Design and Synthesis of Multifunctional Materials Based on an Ionic-Liquid Backbone. *Angew. Chem., Int. Ed.* **2006**, *45*, 5867−5870.
(35) Wu, B.; Hu, D.; Kuang, Y.; Liu, B.; Zhang, X.; Chen, J. Functionalization of Carbon Nanotubes by an Ionic-Liquid Polymer: Dispersion of Pt and PtRu Nanoparticles on Carbon Nanotubes and Their Electrocatalytic Oxidation of Methanol. *Angew. Chem., Int. Ed.* **2009**, *48*, 4751−4754.
(36) Leng, Y.; Wang, J.; Zhu, D.; Ren, X.; Ge, H.; Shen, L. Heteropolyanion-Based Ionic Liquids: Reaction-Induced Self Separation Catalysts for Esterification. *Angew. Chem., Int. Ed.* **2009**, *48*, 168−171.
(37) Leng, Y.; Wang, J.; Zhu, D.; Zhang, M.; Zhao, P.; Long, Z.; Huang, J. Polyoxometalate-Based Amino-Functionalized Ionic Solid Catalysts Lead to Highly Efficient Heterogeneous Epoxidation of Alkenes with H_2O_2. *Green. Chem.* **2011**, *13*, 1636−1639.
(38) Zhao, P.; Wang, J.; Chen, G.; Zhou, Y.; Huang, J. Phase-Transfer Hydroxylation of Benzene with H_2O_2 Catalyzed by a Nitrile-Functionalized Pyridinium Phosphovanadomolybdate. *Catal. Sci. Technol.* **2013**, *3*, 1394−1404.
(39) Long, Z.; Zhou, Y.; Chen, G.; Zhao, P.; Wang, J. 4,4′-Bipyridine-Modified Molybdovanadophosphoric Acid: A Reusable Heterogeneous Catalyst for Direct Hydroxylation of Benzene with O_2. *Chem. Eng. J.* **2014**, *239*, 19−25.
(40) Chen, G.; Zhou, Y.; Zhao, P.; Long, Z.; Wang, J. Mesostructured Dihydroxy-Functionalized Guanidinium-Based Polyoxometalate with Enhanced Heterogeneous Catalytic Activity in Epoxidation. *ChemPlusChem* **2013**, *78*, 561−569.
(41) Demberelnyamba, D.; Yoon, S. J.; Lee, H. New Epoxide Molten Salts: Key Intermediates for Designing Novel Ionic Liquids. *Chem. Lett.* **2004**, *33*, 560−561.
(42) Bates, E. D.; Mayton, R. D.; Ntai, I.; Davis, J. H. CO_2 Capture by a Task-Specific Ionic Liquid. *J. Am. Chem. Soc.* **2002**, *124*, 926−927.
(43) Misono, M. Heterogeneous Catalysis by Heteropoly Compounds of Molybdenum and Tungsten. *Catal. Rev.: Sci. Eng.* **1987**, *29*, 269−321.
(44) David, J. H.; Phillip, K. K.; Ang, M. T. C.; Chen, L.; James, E. R.; Clement, R. Y.; Philip, G. J. Reversible Zwitterionic Liquids, the Reaction of Alkanol Guanidines, Alkanol Amidines, and Diamines with CO_2. *Green Chem.* **2010**, *12*, 713−721.
(45) Okuhara, T.; Nakato, T. Catalysis by Porous Heteropoly Compounds. *Catal. Surv. Jpn.* **1998**, *2*, 31−44.
(46) Vasylyer, M. V.; Neumann, R. New Heterogeneous Polyoxometalate Based Mesoporous Catalysts for Hydrogen Peroxide Mediated Oxidation Reactions. *J. Am. Chem. Soc.* **2004**, *126*, 884−890.
(47) Kalita, A. C.; Marchal, C. R.; Murugavel, R. Cationic D4R Zinc Phosphate-Anionic Polyoxometalate Hybrids: Synthesis, Spectra, Structure and Catalytic Studies. *Dalton Trans.* **2013**, *42*, 9755−9763.
(48) Liu, F.; Kong, W.; Qi, C.; Zhu, L.; Xiao, F. Design and Synthesis of Mesoporous Polymer-Based Solid Acid Catalysts with Excellent Hydrophobicity and Extraordinary Catalytic Activity. *ACS Catal.* **2012**, *2*, 565−572.
(49) Rozner, D. S.; Alsters, P. L.; Neumann, R. A Water-Soluble and "Self-Assembled" Polyoxometalate as a Recyclable Catalyst for Oxidation of Alcohols in Water with Hydrogen Peroxide. *J. Am. Chem. Soc.* **2003**, *125*, 5280−5281.
(50) Ma, B.; Zhang, Y.; Ding, Y.; Zhao, W. A Water-Soluble Dilacunary Silicotungstate as an Effective Catalyst for Oxidation Alcohols in Water with Hydrogen Peroxide. *Catal .Commun.* **2010**, *11*, 853−857.
(51) Karimi, B.; Behzadnia, H.; Bostina, M.; Vali, H. A Nano-Fibrillated Mesoporous Carbon as an Effective Support for Palladium Nanoparticles in the Aerobic Oxidation of Alcohols on Pure Water. *Chem.—Eur. J.* **2012**, *18*, 8634−8640.
(52) Lang, X.; Li, Z.; Xia, C. $[\alpha\text{-}PW_{12}O_{40}]^{3-}$ Immobilized on Ionic Liquid-Modified Polymer as a Heterogeneous Catalyst for Alcohol Oxidation with Hydrogen Peroxide. *Synth. Commun.* **2008**, *38*, 1610−1616.
(53) Leng, Y.; Zhao, P.; Zhang, M.; Wang, J. Amino Functionalized Bipyridine-Heteropolyacid Ionic Hybrid: A Recyclable Catalyst for Solvent-Free Oxidation of Benzyl Alcohol with H_2O_2. *J. Mol. Catal. A: Chem.* **2012**, *358*, 67−72.
(54) Pourjavadi, A.; Hosseini, S. H.; Moghaddam, F. M.; Foroushani, B. K.; Bennett, C. Tungstate Based Poly(ionic liquid) Entrapped Magnetic Nanoparticles: A Robust Oxidation Catalyst. *Green Chem.* **2013**, *15*, 2913−2919.
(55) Katryniok, B.; Kimura, H.; Skrzyńska, E.; Girardon, J.; Fongarland, P.; Capron, M.; Ducoulombier, R.; Mimura, N.; Paul, S.; Dumeignil, F. Selective Catalytic Oxidation of Glycerol: Perspectives for High Value Chemicals. *Green Chem.* **2011**, *13*, 1960−1979.
(56) Frassoldati, A.; Pinel, C.; Besson, M. Promoting Effect of Water for Aliphatic Primary and Secondary Alcohol Oxidation over Platinum Catalysts in Dioxane/Aqueous Solution Media. *Catal. Today* **2011**, *173*, 81−88.
(57) Chibani, S.; Michel, C.; Delbecq, F.; Pinel, C.; Besson, M. On the Key Role of Hydroxyl Groups in Platinum-Catalysed Alcohol Oxidation in Aqueous Medium. *Catal. Sci. Technol.* **2013**, *3*, 339−350.
(58) Jung, Y.; Marcus, R. A. On the Theory of Organic Catalysis "on Water. *J. Am. Chem. Soc.* **2007**, *129*, 5492−5502.
(59) Duncan, D. C.; Chambers, R. C.; Hecht, E.; Hill, C. L. Mechanism and Dynamics in the $H_3[PW_{12}O_{40}]$-Catalyzed Selective Epoxidation of Terminal Olefins by H_2O_2. Formation, Reactivity, and Stability of $\{PO_4[WO(O_2)_2]_4\}^{3-}$. *J. Am. Chem. Soc.* **1995**, *117*, 681−691.
(60) Zhang, S.; Zhao, G.; Gao, S.; Xi, Z.; Xu, J. Secondary Alcohols Oxidation with Hydrogen Peroxide Catalyzed by $[n\text{-}C_{16}H_{33}N(CH_3)_3]_3PW_{12}O_{40}$: Transform-and-Retransform Process between Catalytic Precursor and Catalytic Activity Species. *J. Mol. Catal. A: Chem.* **2008**, *289*, 22−27.